

Nuclear-spin relaxation due to translational diffusion in a hexatic-*B* and crystalline-*B* phase

S. Žumer

Department of Physics, E. Kardelj University of Ljubljana, Jadranska 19, 61000 Ljubljana, Yugoslavia

M. Vilfan

J. Stefan Institute, E. Kardelj University of Ljubljana, 61000 Ljubljana, Yugoslavia

(Received 15 February 1983)

The general theory of nuclear-spin relaxation induced by translational self-diffusion in liquid crystals, developed in previous papers, is applied to the crystalline-*B* and hexatic-*B* phases of smectics by taking into account their characteristic features concerning molecular positional ordering, the inter- and intralayer molecular jumps, and the correlation in the layer stacking. The evaluated anisotropy and dispersion of T_1 and $T_{1\rho}$ are presented graphically for a variety of parameters. It is shown that in most cases $T_{1\rho}$, due to translational diffusion, has a characteristic anisotropy and dispersion while T_1 is expected to be nearly isotropic and with ω^2 -type dispersion at usual NMR frequencies. The relaxation study cannot discriminate between various types of the interlayer and intralayer correlations occurring in the crystalline-*B* and hexatic-*B* phases of the smectics except in the case when relative layer motions are fast compared to the diffusion. The comparison of the theoretical relation and experimental data enables the determination of diffusion constant D_1 in the smectic-*B* phases while the ratio $D_1/D_{||}$ could be determined only via precise study of the $T_{1\rho}$ angular dependence. With the application of the theory to available T_1 data of the smectic-*B* phase of N-[4-(*n*-dodecanoyl)benzylidene]-4'-aminoazobenzene (C_{12} BAA) and of the smectic- B_c phase of terephthal-bis(4-*n*-butylaniline) (TBBA), the corresponding D_1 are estimated.

I. INTRODUCTION

Nuclear-spin relaxation studies have considerably increased the insight into the molecular dynamics of liquid-crystalline phases. So far rather complete studies have been devoted to the nematic phase^{1,2} and smectic-*A* phase,³⁻⁵ while nuclear magnetic relaxation phenomena in the three-dimensional (3D) ordered smectic phases are far less known.^{4,6-9} These phases recently attracted a lot of interest as possible model systems where 2D melting process¹⁰⁻¹² can be studied.

Smectic-*B* phase is characterized by regularly stacked layers in which molecules are arranged in a two-dimensional hexagonal lattice with their long axes being perpendicular to the plane of the layer (Fig. 1). X-ray studies¹³⁻¹⁵ have confirmed the existence of two kinds of smectic-*B* phases: the crystalline-*B* phase,¹³ where intralayer positional order of molecules has long range similarly as in some tilted ordered phases,^{16,17} and hexatic-*B* phase,^{11,12} where intralayer positional order has a short range (only about 20 molecular diameters¹⁵) while bond orientations¹¹ retain the long-range order.

Smectic mesophases are strongly anisotropic systems where interlayer interactions are weak. In the crystalline-*B* phase resulting interlayer correlations strongly depend on the length of the aliphatic tails,¹⁶ preparation of the sample, and the state of annealing.¹³ Layers can be stacked¹³ at random (no correlation), or with partial correlation extending from zero to ten molecular lengths where the layers are arranged in monolayers (*A,A,A*, . . .), in bilayers (*A,B,A,B*, . . .), in trilayers (*A,B,C*, . . .), or in more complicated structures. These systems have small but nonzero elastic shear modulus C_{44} .^{18,19} In the

hexatic-*B* phase which exists only as an intermediate mesophase (after a 2D melting) between crystalline-*B* and smectic-*A* phase, thermal fluctuations via uncorrelated layer displacements completely smear out interlayer correlations.¹⁵ Up to now there is no conclusive information about these relative layer (sliding) motions²⁰ and their relation to the interlayer correlations. Because of the anisotropy of phenyl rings a local intralayer orientational ordering of the herringbone type^{14,15,17,21,22} develops in both phases. The correlation length of this ordering is limited by the positional correlation length, while its dynamics is determined by molecular rotations around their long axes. These hindered rotations with six energetically equivalent positions⁶ are relatively fast ($\sim 10^{11}$ sec⁻¹) (Ref. 23) and partially correlated due to the relative positions of the phenyl rings of the neighboring molecules¹⁷ in the herringbone structure.

The orientational fluctuations of long molecular axes have a characteristic frequency $\sim 10^{10}$ sec⁻¹ (Ref. 23) but much smaller amplitudes than in the high-temperature smectic phases.⁶ "Head-to-tail" reorientations of 180° around the short molecular axes²⁴ are very slow ($\sim 10^4$ sec⁻¹).

In spite of the high positional order of the molecules in the ordered smectic phases there are fast local motions with large amplitudes (≥ 2 Å) (Ref. 17) and molecular translational diffusion which is a slow jump process ($\sim 10^6$ sec⁻¹) as in solids but with much weaker dynamical correlations. Diffusion constants have been determined by direct NMR measurements only close to the smectic-*B*—smectic-*A* transition^{7,25} and by quasielastic neutron scattering²⁶ and tracer method.²⁷ Their values are of the order 10^{-11} – 10^{-14} m²/sec with small anisotropy

($D_{\perp}/D_{\parallel} \approx 2$). The intralayer jump rate is thus about 100 times greater than the interlayer jump rate.

The investigations of molecular dynamics by nuclear magnetic relaxation require a precise knowledge of contributions of different types of molecular motion to the magnetic relaxation rate. In our first paper,²⁸ hereafter called I, we described the general theory of the longitudinal spin relaxation due to translational self-diffusion in thermotropic liquid crystals and applied it to the nematic phase. It was shown that Torrey's approach²⁹ for classical liquids is a fairly good approximation for T_1 frequency dependence in nematic phases. In our second paper,³⁰ hereafter called II, we applied the theory to the smectic-*A* phase, where the isotropic Torrey's approach cannot be used.

In this paper we present—on the basis of the previous works (I and II)—the calculation of the diffusion induced magnetic spin relaxation rate in the smectic-*B* phases. A theoretical treatment for both crystalline-*B* and hexatic smectic-*B* phase where different positional correlations are taken into account, is presented in Sec. II. Numerical results for T_1^{-1} and $T_{1\rho}^{-1}$ are presented graphically and discussed together with the available experimental data in the Sec. III.

II. THEORY

A. Model and assumptions

In our treatment of the proton magnetic relaxation rate caused by translational diffusion we neglect all details which do not play an important role in this relaxation process. Therefore, the following simplified model of the smectic-*B* phase is adopted.

(i) Molecules are effectively represented by rigid cylinders with length l and diameter d , having resonant nuclei (protons with $I = \frac{1}{2}$) distributed along the long molecular axis.²⁸ The long molecular axes are assumed to be perfectly oriented in the direction perpendicular to the layer [the measured order parameter is close to 1 (Ref. 6)]. This model with motionally averaged shape and magnetic interaction is justified because both local orientational fluctuations of the long molecular axis²³ and rotations²³ around it are fast while head-to-tail reorientations²⁴ are slow in the time scale which is determined by magnetic dipolar interaction and self-diffusion jump rate. Similarly fast fluctuations around equilibrium molecular positions contribute to the nuclear magnetic relaxation only via interaction averaging, so that molecular centers are taken to be arranged in the two-dimensional hexagonal lattice with the lattice constant equal to d (see Fig. 1). This assumption is appropriate even for hexatic-*B* phase as intralayer positional correlation lengths are always long compared to the range of the magnetic dipolar interactions.

(ii) Smectic layers are regularly stacked in a one-dimensional array with the lattice constant equal to the length of the molecule l . As the possible interlayer ordering^{13–16} varies from zero to complete correlation we shall make the calculation of T_1^{-1} for three possibilities: (a) complete order with *AAA* . . . stacking, which would be appropriate for the description of the crystalline-*B* phase with such stacking, (b) complete static disorder, which can be applied for crystalline-*B* or hexatic-*B* phase, and (c) complete dynamic disorder fast in the time scale of the

jump diffusion (10^6 – 10^8 Hz). This can be used in the case of fast layer sliding in the hexatic-*B* phase.

(iii) Translational diffusion of the molecules is described—similarly as in the smectic-*A* phase—by two independent thermally activated jump motions:

(a) intralayer random jump process in the two-dimensional hexagonal lattice where only six nearest lattice points are accessible in one jump. The jump length equals d . This motion depends only on the local structure, so it is not affected by the transition from the crystalline-*B* to hexatic-*B* phase because the intralayer correlation length remains long compared to the jump length d .

(b) interlayer random jump process where a jump terminates in one of the two adjacent layers. The possible lateral displacement to one of the nearest lattice points in these adjacent layers depends on the relative position of the layers (interlayer correlation). The jump length varies between l and $(l^2 + d^2)^{1/2}$.

The average time needed for one jump is, as in Torrey's model,²⁹ negligible compared to the average time interval between two successive intralayer (τ_{\perp}) or interlayer (τ_{\parallel}) jumps. Each molecule is taken to move independently. Positional two-molecular correlations will be included only via static pair correlations,^{28,29} while dynamical pair correlations, which are usually taken into account in solids,³¹ will be neglected. This is expected to be justified because local positional motions in ordered smectic phases have much larger amplitudes¹⁷ as in solids.

B. Nuclear magnetic relaxation

In our calculations of the relaxation rates T_1^{-1} and $T_{1\rho}^{-1}$ due to molecular self-diffusion in the smectic-*B* phases we further take into account that other molecular motions have characteristic correlation times essentially different from τ_{\perp} and τ_{\parallel} . So the relaxation induced by self-diffusion can be treated independently and is effected by the rest of the molecular dynamics only via averaging effects. The relaxation process is single exponential and described by the well-known relaxation rate³²:

$$T_1^{-1} = \frac{3}{2} \gamma^4 \hbar^2 I(I+1) [J^{(1)}(\omega, \Delta) + J^{(2)}(2\omega, \Delta)] \quad (1)$$

in the laboratory frame, and by

$$T_{1\rho}^{-1} = \frac{3}{8} \gamma^4 \hbar^2 I(I+1) [J^{(0)}(2\omega_1, \Delta) + 10J^{(1)}(\omega, \Delta) + J^{(2)}(2\omega, \Delta)] \quad (2)$$

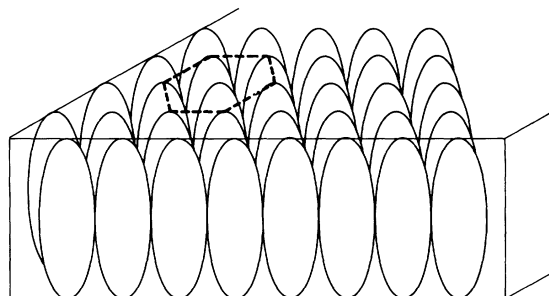


FIG. 1. Schematic presentation of the smectic-*B* structure.

in the rotating frame. Here $J^{(k)}(\omega, \Delta)$ are the spectral densities³² of the spatial part of the dipolar interaction at frequency ω for the case when the angle between the magnetic field and the normal to the smectic layers equals Δ . $J^{(k)}(\omega, \Delta)$ are related to the spectral densities $J^{(k)}(\omega)$, which stand for $\Delta=0$, through a simple relation.²⁸ The formal form of T_1^{-1} and $T_{1\rho}^{-1}$ given by Eqs. (1) and (2) can be used either if translational self-diffusion rate is slow or fast compared to the intermolecular dipolar coupling ω_D ($\sim 10^5$ Hz). In the first case, the intermolecular magnetic interactions are not motionally averaged and a common spin temperature of the layer is established in a time much shorter than T_1 , which enables the use of the spin temperature approximation.³² In the second case, intermolecular dipolar interactions are averaged out. The relaxation of each molecule should be treated separately as in usual polyatomic liquids, but one obtains equations of the form (1) and (2) again if three spin correlations are neglected.³³

It has been shown in I that the diffusional part of the spectral densities $J^{(k)}(\omega)$ of the 3D liquid crystal can be written as the following integral over the 3D \vec{q} space:

$$J^{(k)}(\omega) = (n/16\pi^3) \int \text{Re}[\mathcal{F}_{\xi}^{(k)*}(\vec{q}) \mathcal{F}_{0\xi}^{(k)}(q)]_{\xi} \times S_s(\vec{q}, \omega/2) d^3q. \quad (3)$$

In Eq. (3) n is the density of the resonant nuclei with spin I . **Functions**

$$\mathcal{F}_{\xi}^{(k)}(\vec{q}) = \int F_{\xi}^{(k)}(\vec{r}) g(\vec{r}) e^{i\vec{q} \cdot \vec{r}} d^3r \quad (4)$$

and

$$\mathcal{F}_{0\xi}^{(k)}(\vec{q}) = \int F_{\xi}^{(k)}(\vec{r}) g_0(\vec{r}) e^{i\vec{q} \cdot \vec{r}} d^3r \quad (5)$$

are Fourier transforms of the spatial part of the dipolar interaction³¹

$$F_{\xi}^{(k)}(\vec{r}) = \frac{e^{ik\phi}}{[\rho^2 + (z + \xi)^2]^{5/2}} \times \begin{cases} \rho^2 - 2(z - \xi)^2 & k=0 \\ \rho(z - \xi), & k=\pm 1 \\ \rho^2, & k=\pm 2 \end{cases} \quad (6)$$

weighted by $g(\vec{r})$ (static pair correlation function) or with $g_0(\vec{r})$ (short-range part of the static pair correlation function), respectively. The coordinates ρ, z, ϕ are cylindrical coordinates of the vector connecting centers of two molecules, which carry the i th and j th interacting spins. ξ is the difference between the distances ξ_i and ξ_j which measure the relative positions of the i th and j th spin in the corresponding molecules (Fig. 2). The average indicated by the subscript ξ is performed with the distribution $W(\xi)$, which is the convolution of two uniform effective distributions of the resonant nuclei along the molecular axis. This distribution will be specified by a parameter a which stands for the distance of the closest approach of two nuclei belonging to two adjacent layers (Fig. 2). $W(\xi)$ is given in detail in I and II. The dynamical structure fac-

tor $S_s(\vec{q}, \omega)$ which contains all information on the diffusional motion of molecules will be described in the next section.

It should be mentioned that the motional averaging of the interlayer magnetic interactions due to the fast relative layer sliding would result in a 2D integration instead of 3D in Eq. (3) as shown in the Appendix.

C. Dynamical structure factor $S_s(\vec{q}, \omega)$

This $S_s(\vec{q}, \omega)$ is the space-time Fourier transform of the one-particle dynamical autocorrelation function $G_s(\vec{r}, t)$. Function $G_s(\vec{r}, t)$ represents, when multiplied by d^3r , the probability that a molecule, which is initially at the origin, is located in d^3r at \vec{r} after a time t . Following Chandrasekhar's treatment³⁴ adapted to the smectic systems (see II) one can in the NMR frequency range²⁸ easily find

$$S_s(\vec{q}, \omega) = \frac{2\tau_{\vec{q}}}{1 + (\omega\tau_{\vec{q}})^2}, \quad (7)$$

with

$$\tau_{\vec{q}}^{-1} = \frac{1 - A_{\perp}(\vec{q})}{\tau_{\perp}} + \frac{1 - A_{\parallel}(\vec{q})}{\tau_{\parallel}}, \quad (8)$$

where A_{\perp} and A_{\parallel} are Fourier transforms of the molecular distribution after a single jump in the perpendicular or parallel direction, respectively. They depend on the details of the diffusion process. Because intralayer positional correlations are in both hexatic- and crystalline- B phases much longer than a jump length we have assumed in our model the same intralayer jump process for cases (a)–(c) of interlayer correlation. Taking into account the hexagonal structure and representing the vector \vec{q} with cylindrical coordinates $q_{\perp}, \varphi, q_{\parallel}$ one gets

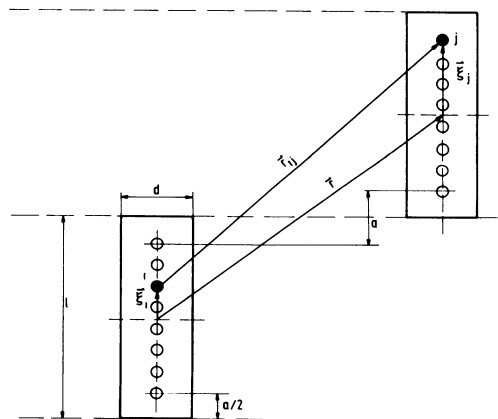


FIG. 2. Schematic presentation of two molecules with notations used in the text.

$$A_{\perp}(\vec{q}) = \frac{1}{3} \sum_{m=1}^3 \cos \left[q_{\perp} d \cos \left[\varphi - m \frac{2\pi}{3} \right] \right]. \quad (9)$$

On the other hand, the interlayer correlation length is much shorter so that we must treat A_{\parallel} for each type of the interlayer correlation separately as follows.

(a) Completely ordered layer packing. Here a molecule can jump to one of the two adjacent layers and takes place on one of the seven nearest possible positions in each layer. The resulting Fourier transform is given by

$$A_{\parallel}(\vec{q}) = \frac{1}{7} \cos(q_{\parallel} l) [1 + 6A_{\perp}(\vec{q})]. \quad (10)$$

(b) Complete static disorder of the layer stacking. In this case possible molecular positions in each adjacent layer which is accessible with one interlayer jump lay approximately within a circle having a radius d . So one finds

$$A_{\parallel}(\vec{q}) = 2 \cos(q_{\parallel} l) J_1(q_{\perp} d) / (q_{\perp} d). \quad (11)$$

Here J_1 is the Bessel function of first order.

(c) Complete dynamic disorder of the layer stacking. Here the layer sliding is assumed to be faster than intralayer translational diffusion, so the correlation is lost when a molecule jumps to the adjacent layer. Therefore, the relaxation rate depends only on the decay of the intralayer correlations what can be formally described by $A_{\parallel} = 0$ (see the Appendix).

The average times between random jumps in the direction parallel to the molecular director (τ_{\parallel}) and perpendicular to the molecular director (τ_{\perp}) are related to the macroscopic diffusion coefficients through²⁸⁻³⁰

$$D_{\perp} = d^2 / (4\tau_{\perp}), \quad (12)$$

$$D_{\parallel} = l^2 / (2\tau_{\parallel}), \quad (13)$$

where D_{\perp} and D_{\parallel} stand for the eigenvalues of the diffusion tensor in the perfectly oriented smectic- B phase.

D. Static pair correlation functions

Using our simplified models of the smectic- B phases we construct static pair correlation function in such a way that the regular stacking of the layers, two-dimensional hexagonal lattice within the layers, and interlayer correlations are described.

$$\mathcal{F}_{0\xi}^{(k)}(\vec{q}) = 2\pi i^k e^{ik\varphi} \begin{pmatrix} 1 \\ i/3 \\ 1/3 \end{pmatrix} \frac{q_{\parallel}^2}{q_{\parallel}^2 + q_{\perp}^2} [q_{\parallel} d K_{k-1}(q_{\parallel} d) J_k(q_{\perp} d) + q_{\perp} d J_{k-1}(q_{\perp} d) K_k(q_{\parallel} d)] + \frac{1}{q_{\perp} d} J_k(q_{\perp} d) \begin{pmatrix} -2 \\ i \\ 1 \end{pmatrix} \mathcal{S}_k, \quad (20)$$

where three lines of each column correspond to $k=0, 1$, and 2 , respectively, J_k are Bessel functions, K_k are modified Bessel functions, while functions \mathcal{S}_k can be written in the following form:

(a) Completely ordered layer stacking (A, A, A, \dots):

$$g(\vec{r}) = l \times \begin{cases} g_{\perp}(\vec{\rho}) \delta(z), & |z| < l \\ [\sqrt{3}d^2 \delta(\vec{\rho}) + g_{\perp}(\vec{\rho})] \sum_{m=\pm 1}^{\pm \infty} \delta(z - ml), & |z| \geq l. \end{cases} \quad (14)$$

(b) Complete static disorder of the layer stacking (uncorrelated layer positions):

$$g(\vec{r}) = l \times \begin{cases} g_{\perp}(\vec{\rho}) \delta(z), & |z| < l \\ \sum_{m=\pm 1}^{\pm \infty} \delta(z - m), & |z| \geq l \end{cases} \quad (15)$$

with

$$g_{\perp}(\vec{\rho}) = \sqrt{3}d^2 \sum_i \delta(\vec{\rho} - \vec{\rho}_i), \quad (16)$$

where the sum runs over six nearest neighbors. The local part of the static pair correlation function is the same in both cases:

$$g_0(\vec{r}) = \begin{cases} 0, & z=0, \rho < d \\ 1, & |z| > l \text{ and } z=0, \rho > d. \end{cases} \quad (17)$$

(c) Dynamical disorder of the layer stacking: Due to the dynamical disorder of the layer positions there is no positional correlation between molecules belonging to the different layers. The interlayer contribution to the magnetic interaction is therefore averaged out. This is formally taken into account by the vanishing of $g(\vec{r})$ for \vec{r} outside the layer. Therefore,

$$g(\vec{r}) = l \delta(z) g_{\perp}(\vec{\rho}), \quad (18)$$

while the local part is given by

$$g_0(\vec{r}) = l \delta(z) \begin{cases} 0, & \rho < d \\ 1, & \rho \geq d. \end{cases} \quad (19)$$

E. Relaxation rates T_{\perp}^{-1} and T_{\parallel}^{-1}

In order to obtain the relaxation rates T_{\perp}^{-1} and T_{\parallel}^{-1} Fourier transforms of dipolar interaction, $\mathcal{F}_{0\xi}^{(k)}(\vec{q})$ and $\mathcal{F}_{\xi}^{(k)}(\vec{q})$, defined by Eqs. (4)–(6), should be evaluated according to the different forms of g and g_0 .

In the case of static layer packing where g_0 is given by (17), the evaluation of function $\mathcal{F}_{0\xi}^{(k)}(\vec{q})$ is performed in the same way as in nematics and described in detail in I. The result for cases (a) and (b) is given by

$$\begin{aligned}
\mathcal{S}_1 &= \frac{1}{2} \cos[q_{\parallel}(l-\xi)] \left[\frac{d}{l-\xi} \right]^2 - q_{\parallel} d \left[\cos[q_{\parallel}(l-\xi)] \left[\frac{d}{l-\xi} \right] - q_{\parallel} d \operatorname{Ci}[q_{\parallel}(l-\xi)] \right], \\
\mathcal{S}_2 &= -\frac{1}{3} \sin[q_{\parallel}(l-\xi)] \left[\frac{d}{l-\xi} \right]^3 + \frac{1}{3} q_{\parallel} d \mathcal{S}_1, \\
\mathcal{S}_3 &= \frac{1}{4} \cos[q_{\parallel}(l-\xi)] \left[\frac{d}{l-\xi} \right]^4 - \frac{1}{4} q_{\parallel} d \left[\frac{1}{3} \cos[q_{\parallel}(l-\xi)] \left[\frac{d}{l-\xi} \right]^3 - \frac{1}{3} q_{\parallel} d \mathcal{S}_1 \right],
\end{aligned} \tag{21}$$

with Ci as the integral cosine.

In the case of dynamical disorder due to fast layer sliding [case (c)] $\mathcal{F}_{0\xi}^{(k)}(\vec{q})$ depends only on \vec{q}_{\perp} and cannot be evaluated in a closed analytical form. It can be expressed by

$$\mathcal{F}_{0\xi}^{(k)}(\vec{q}_{\perp}) = 2\pi i^k e^{ik\varphi} \int_a^{\infty} J_k(\rho q_{\perp}) \left[\frac{\rho^2 - 2\xi^2}{\rho\xi} \right] \frac{\rho}{(\rho^2 + \xi^2)^{5/2}} d\rho. \tag{22}$$

In the evaluation of $\mathcal{F}_{\xi}^{(k)}(\vec{q})$ three different static pair correlation functions [Eqs. (14), (15), and (18)] are taken into account:

(a) completely ordered layer stacking,

$$\begin{aligned}
\mathcal{F}_{\xi}^{(k)}(\vec{q}) &= f_{\xi}^{(k)}(\vec{q}_{\perp}) + \sqrt{3} l d^2 \left[-2 \begin{bmatrix} 1 \\ 0 \\ 0 \end{bmatrix} \left(\frac{e^{iq_{\parallel}l}}{(l+\xi)^3} + \frac{e^{-iq_{\parallel}l}}{(l-\xi)^3} \right) + \frac{e^{-iq_{\parallel}l}}{[d^2 + (l-\xi)^2]^{5/2}} \begin{bmatrix} d^2 - 2(l-\xi)^2 \\ d(\xi-l) \\ d^2 \end{bmatrix} \right. \\
&\quad \left. + \frac{e^{iq_{\parallel}l}}{[d^2 + (l+\xi)^2]^{5/2}} \begin{bmatrix} d^2 - 2(l+\xi)^2 \\ d(\xi+l) \\ d^2 \end{bmatrix} \right] \sum_{m=1}^3 e^{i2\pi km/3} e^{iq_{\perp}d \cos(\varphi - 2\pi m/3)}, \tag{23}
\end{aligned}$$

(b) disordered stacking,

$$\mathcal{F}_{\xi}^{(k)}(\vec{q}) = f_{\xi}^{(k)}(\vec{q}_{\perp}) - 4\pi \begin{bmatrix} 1 \\ \frac{1}{3} \\ \frac{1}{3} \end{bmatrix} e^{ik\varphi} q_{\perp} l e^{-lq_{\perp}} \left[\cos(q_{\parallel}l) \begin{bmatrix} \cosh \xi q_{\perp} \\ i \sinh \xi q_{\perp} \\ \cosh \xi q_{\perp} \end{bmatrix} + \sin(q_{\parallel}l) \begin{bmatrix} i \sinh \xi q_{\perp} \\ \cosh \xi q_{\perp} \\ i \sinh \xi q_{\perp} \end{bmatrix} \right], \tag{24}$$

(c) dynamically disordered layer stacking,

$$\mathcal{F}_{\xi}^{(k)}(\vec{q}) = f_{\xi}^{(k)}(\vec{q}), \tag{25}$$

where the common part $f_{\xi}^{(k)}(\vec{q})$ is given by

$$f_{\xi}^{(k)}(\vec{q}) = \sqrt{3} \frac{d^2 l}{(d^2 + \xi^2)^{5/2}} \begin{bmatrix} d^2 - 2\xi^2 \\ d \\ d^2 \end{bmatrix} \sum_{m=1}^3 e^{i2\pi km/3} \exp[iq_{\perp}d \cos(\varphi - 2\pi m/3)]. \tag{26}$$

To obtain finally the relaxation rates T_1^{-1} and $T_{1\rho}^{-1}$ integration over \vec{q} space and averaging over ξ have been performed numerically. Introducing dimensionless functions $P_1(\omega\tau_1, D_{\perp}/D_{\parallel}, l/d, a/d, \Delta)$ and $P_{1\rho}(\omega\tau_1, \omega_1\tau_1, D_{\perp}/D_{\parallel}, l/d, a/d, \Delta)$ one can write

$$T_1^{-1} = \alpha \tau_1 P_1 \tag{27}$$

and

$$T_{1\rho}^{-1} = \frac{1}{4} \alpha \tau_1 P_{1\rho}, \tag{28}$$

where

$$\alpha = \frac{9}{8} \gamma^4 \hbar^2 n / d^3 \tag{29}$$

measures the strength of the intermolecular dipolar interactions. The dependences of functions P_1 and $P_{1\rho}$ on characteristic parameters are discussed in the next section for all three types of correlation.

III. RESULTS AND DISCUSSION

The functions $P_{1\rho}$ and P_1 have been numerically evaluated for all three types of the interlayer correlations (a)–(c) in the frequency range $\omega\tau_1=0$ to $\omega\tau_1=40$ for a number of different values of D_{\perp}/D_{\parallel} , a , ω_1 , and Δ . As τ_1 is usually of the order 10^{-6} sec the above frequency range covers typical proton NMR frequencies ω between 1 and 300 MHz and frequencies ω_1 for $T_{1\rho}$ measurements between 30 and 300 kHz.

In our calculations a uniform distribution of spins along the molecular axis has been assumed. The quantity a (see Fig. 2) measures the distance of closest approach between two nuclei belonging to two neighboring molecules lying in two adjacent layers. This distribution was proved in II to present a good approximation. Figure 3 shows for crystalline-*B* and hexatic *B*—cases (a) and (c)—the dependence of P_1 on the distance a for $\Delta=0^\circ$ and 90° . Starting

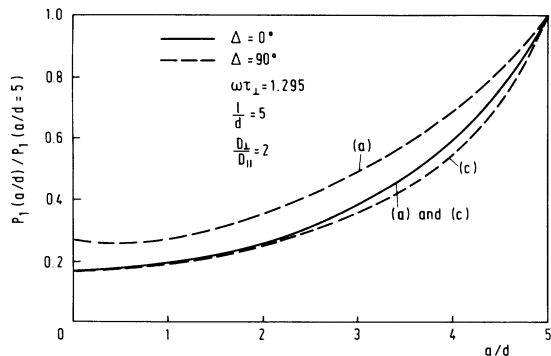


FIG. 3. Plot of the function P_1 vs a/d for cases (a) and (c).

from $a=l$, what corresponds to a case where all resonant spins are in the center of the molecule, the relaxation rates decrease with decreasing a until for $a \approx d$, P_1 becomes nearly constant. In case (a) and $\Delta \neq 0^\circ$ P_1 begins to increase for $a/d \approx 0.2$ because of the increasing interlayer interaction. One can conclude that for a smectic- B phase where $a \approx 2 \text{ \AA}$ the value of P_1 is rather insensitive to the precise choice of a .

In our further detailed investigation of the frequency dependences of functions P_1 and $P_{1\rho}$ we choose the following molecular parameters: $l/d=5$ and $a/d=0.5$. Figure 4 presents frequency dependences of the spectral densities $J^{(0)}(\omega)$, $J^{(1)}(\omega)$, and $J^{(2)}(\omega)$ for our three types of the interlayer correlation (a), (b), and (c) using $D_\perp/D_\parallel=2$. It is important to note that the difference between spectral densities belonging to the two kinds of the static correla-

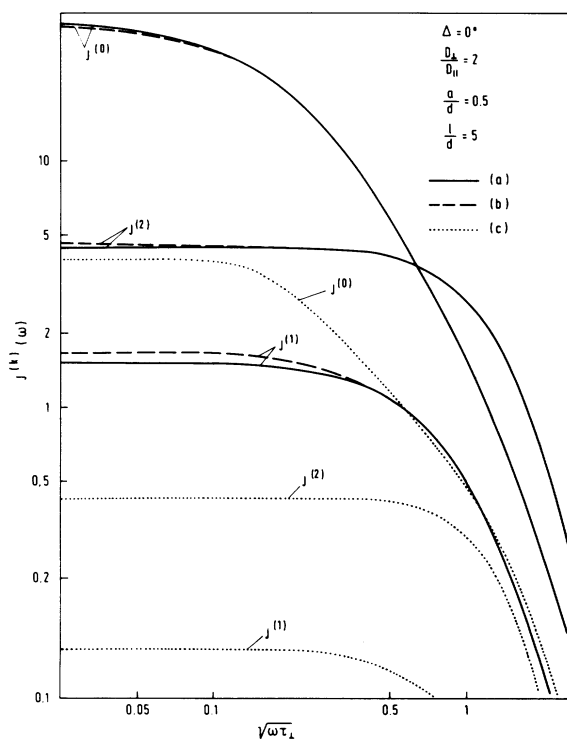


FIG. 4. Dispersion of the spectral densities $J^{(0)}(\omega)$, $J^{(1)}(\omega)$, and $J^{(2)}(\omega)$ for different types of layer packing: (a) complete correlation (solid curve), (b) static disorder (dashed curve), and (c) dynamic disorder (dotted curve).

tion (a) and (b), is negligible, smaller than a few percent, even at low frequencies. Therefore, studying the behavior of the T_1 and $T_{1\rho}$ one cannot make any conclusions about the degree of the interlayer correlation in the crystalline- B and hexatic- B phases, and about 2D melting transition. On the other hand, a kind of the hexatic- B phase (c) where relative layer sliding would be fast compared to the intralayer diffusion, would be relatively easy detected via appreciably different dispersion of $J^{(k)}(\omega)$. In the high-frequency region $\omega\tau_\perp \geq 10$ the spectral densities can be well described by

$$J^{(k)}(\omega) = C^{(k)} \frac{n}{d^3 \omega^2 \tau_\perp}, \quad (30)$$

where

$$C^{(0)} = 0.140, \quad C^{(1)} = 0.044, \quad C^{(2)} = 0.325,$$

for cases (a) and (b), while

$$C^{(0)} = 0.0546, \quad C^{(1)} = 0.0050, \quad C^{(2)} = 0.346$$

for case (c). Here constants $C^{(k)}$ do not depend on parameters d , l , a , and D_\perp/D_\parallel as far as $l \gg d$, $d > a$, and $D_\perp/D_\parallel \geq 1$.

The dispersion of P_1 at $\Delta=90^\circ$ for smectic- B phases in cases (a) and (c) is compared to the dispersion of P_1 for the smectic- A phase and isotropic phase in Fig. 5 where the rates are plotted versus $(\omega\tau_\perp)^{1/2}$. Both smectic phases have $D_\perp/D_\parallel=2$ and $l/d=5$. In the case of the isotropic liquids the diameter of spherical molecules is taken to be equal to our d and $\tau_{\text{iso}} = \tau_\perp$ is used.

The dispersions of P_1 and $P_{1\rho}$ for $\Delta=0^\circ, 90^\circ$ and a polycrystalline sample are presented for cases (a) and (c) in Figs. 6 and 7, respectively. The effect of the ratio D_\perp/D_\parallel on the dispersion of P_1 for $\Delta=0^\circ$ and 90° in cases (a) and (c) is shown in Fig. 8. Inspecting these diagrams the following conclusions can be drawn.

(1) The dispersion of T_1 in the crystalline- B and hexatic- B phase is similar to the dispersion of the smectic- A phase as long as the relative layer motion is not too fast. If in a hexatic- B phase these motions were fast compared to the translational diffusion, the relaxation rate would be appreciably reduced and would have approximately Lorentzian shape in the whole frequency region.

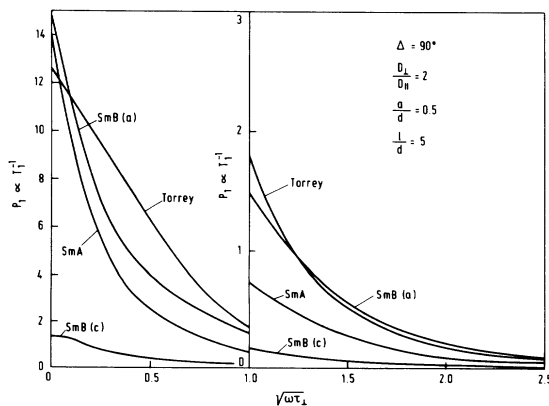


FIG. 5. Dispersion of P_1 for oriented ($\Delta=90^\circ$) smectic- B phases (a), (b), and (c), smectic- A phase, and isotropic liquid (Torrey, Ref. 29).

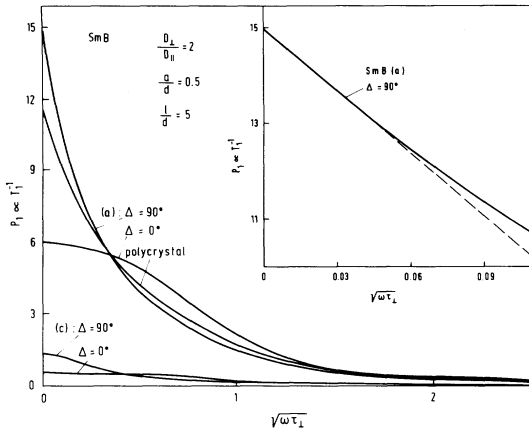


FIG. 6. Dispersion of P_1 for oriented ($\Delta=0^\circ$ and 90°) and polycrystalline sample in cases (a) and (c). The inset shows the comparison of the $c_0 - c_1\omega^{1/2}$ law (dashed line) to the low-frequency behavior of P_1 in case (a).

The comparison with Torrey's curve for isotropic liquids which relatively well describes the whole dispersion of T_1^{-1} in nematics, shows that the use of Torrey's isotropic approach for smectic- B phases is, for $\omega\tau_1 < 1$, a rather poor approximation, but it becomes quite reasonable for $\omega\tau_1 > 2$.

(2) The dispersion curves calculated for the smectic- B phases (a) and (b) follow Torrey's well-known $c_0 - c_1\omega^{1/2}$ frequency dependence^{29,35} only for $\Delta \neq 0$ and $\omega\tau_1 < 10^{-2}$ (see inset in Fig. 6) in contrast to isotropic liquids²⁹ and nematic liquid crystals²⁸ (Torrey's curve in Fig. 5) where this behavior characterizes the usual NMR frequency region. Therefore, this type of frequency behavior could be observed only in $T_{1\rho}$ measurements.

(3) In the high-frequency region with $\omega\tau_1 \geq 10$, which corresponds to the usual NMR frequency range, the self-diffusion induced T_1^{-1} has the ω^{-2} type dispersion and is at $\Delta=0^\circ$ given by

$$T_1^{-1} = 4(C^{(1)} + C^{(2)})\alpha \frac{D_\perp}{d^2\omega^2}, \quad (31)$$

where $C^{(1)}$ and $C^{(2)}$ are given by Eq. (30). Values of T_1 are practically independent of the parameters Δ , l/d , a/d ,

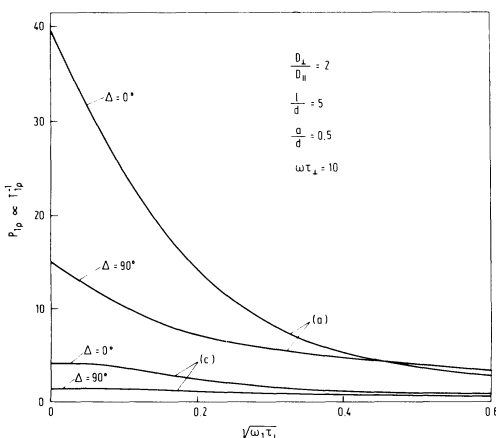


FIG. 7. Dispersion of $P_{1\rho}$ for oriented ($\Delta=0^\circ$ and 90°) sample in cases (a) and (c).

and D_\perp/D_\parallel . Therefore, the measurements of T_1 in the smectic- B phase can provide a simple method for the determination of the diffusion constant D_\perp which is hardly accessible in these systems.

(4) The relaxation rate T_1^{-1} appreciably increases with increasing D_\perp/D_\parallel only at low frequencies. This effect nearly disappears for $\omega\tau_1 > 0.1$, what means that the anisotropy of the translational diffusion can be detected only by T_1 measurements at very low frequencies or by $T_{1\rho}$.

(5) The dependence of P_1 and $P_{1\rho}$ on the orientation of the sample in the magnetic field is pronounced at low frequencies but diminishes as $\omega\tau_1$ becomes larger than 0.1. That is also shown in Figs. 9–11, where the angular dependences of $T_1^{-1}(\Delta)/T_1^{-1}(0^\circ)$ and $T_{1\rho}^{-1}(\Delta)/T_{1\rho}^{-1}(0^\circ)$ for four different frequencies and three different D_\perp/D_\parallel are presented. The anisotropy of T_1 , which amounts to 50% at low frequencies ($\omega\tau_1 \approx 0.01$), is smaller than 10% at higher frequencies ($\omega\tau_1 \geq 0.1$). Therefore, the anisotropy of the diffusion process can be detected only via the detection of the angular anisotropy of $T_{1\rho}$.

It was shown above that diffusion-induced relaxation is rather insensitive to the degree of interlayer correlations and diffusion anisotropy. Therefore, we expect that our results for smectic- B phases can be as well applied to the same process in the tilted ordered smectic phases, where 2D lattices are almost hexagonal.¹⁷

In a comparison of experimental and theoretical predictions for the diffusion-induced relaxation rate, the partial interaction averaging by fast local positional fluctuations¹⁷ must be taken into account. These can be roughly done by introducing an effectively increased lateral distance of the closest approach of the two resonant nuclei belonging to

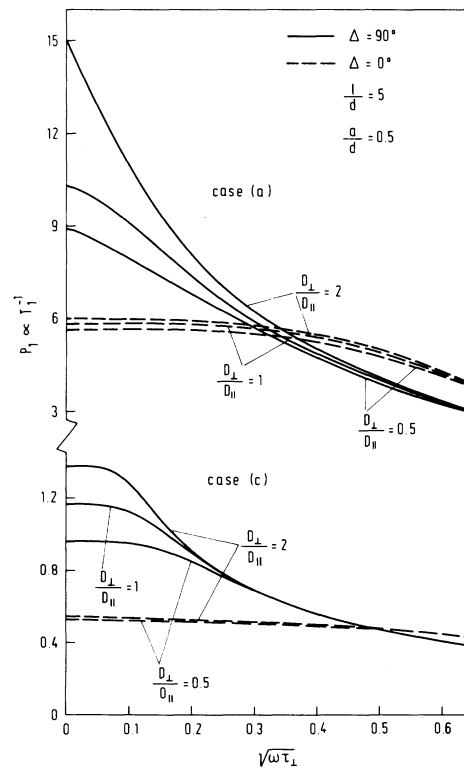


FIG. 8. Comparison between dispersions of P_1 for three different values of D_\perp/D_\parallel in cases (a) and (c) at $\Delta=0^\circ$ and 90° .

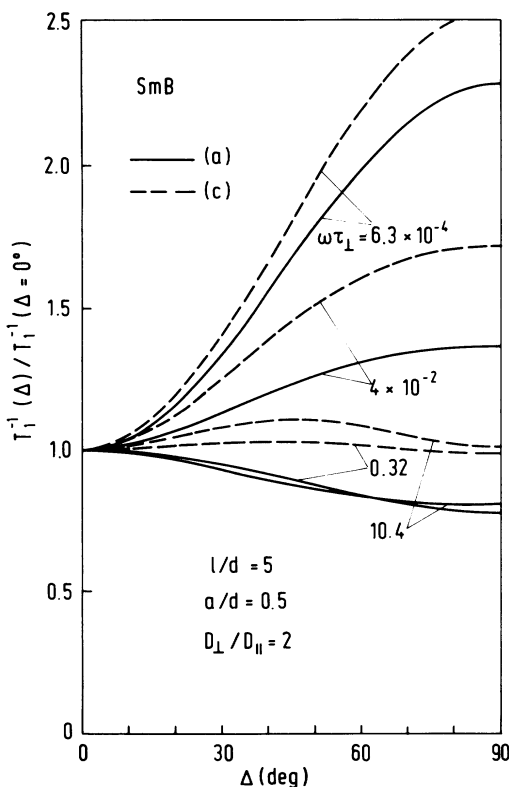


FIG. 9. Angular dependence of T_1^{-1} for four different frequencies in cases (a) and (c).

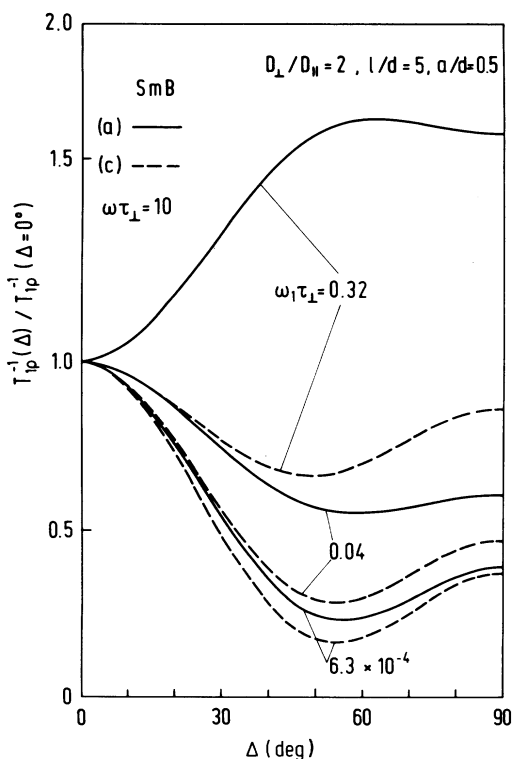


FIG. 10. Angular dependence of T_{1p}^{-1} for three different ω_1 frequencies in cases (a) and (c).

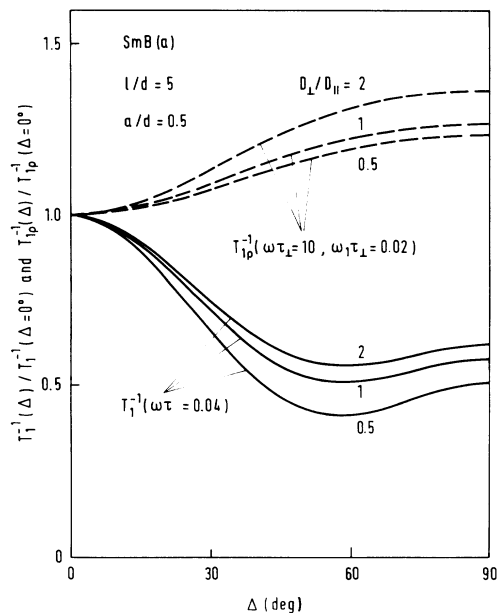


FIG. 11. Angular dependence of T_1^{-1} and T_{1p}^{-1} for three different D_{\perp}/D_{\parallel} in case (a).

the two different molecules. So, instead of α , the effective strength of intermolecular dipolar interactions $\alpha_{\text{eff}} = \alpha(d/d_{\text{eff}})^3$ must be used in Eqs. (27) and (28). The effective distance d_{eff} can be determined from the low-frequency dispersion ($\omega\tau_1 \leq 1$) of the relaxation rate.

In the following we are going to compare our theoretical results with T_1^{-1} dispersion measured by Krüger and co-workers^{7,25} in the smectic- B phase of the N -[4-(n -dodecanoyl)benzylidene]-4'-aminoazobenzene (C_{12} BAA) and to dispersion determined by Blinc *et al.*³ in the smectic- B_c phase of the terephthal-bis-(4- n -butylaniline) (TBBA). In both cases the rough analysis of the T_1 based on Torrey's theory^{3,7,25} clearly showed that translational diffusion is the main relaxational mechanism in the MHz region.

In Fig. 12 it is shown how T_1^{-1} dispersion in C_{12} BAA at 104.3°C can be explained by a sum of a self-diffusion induced relaxation rate $(T_1^{-1})_D$ and a frequency-independent contribution $(T_1^{-1})_R$, possibly due to local molecular reorientations. The best fit of the theoretical curve to the experimental data is obtained for $\tau_1 = 1.3 \times 10^{-6}$ sec, $d_{\text{eff}} = 6.9$ Å, and $(T_1^{-1})_R = 0.66$ sec⁻¹. Here we have additionally used the known data: $l/d \approx 5$, $n = 0.05$ Å⁻³, and $D_{\perp} \approx D_{\parallel}$. The fitted value $d_{\text{eff}} = 6.9$ Å significantly differs from the lattice constant $d = 5.03$ Å (Ref. 21) indicating that there are uncorrelated fast molecular motions with large amplitude (≥ 2 Å). That is in agreement with the x-ray studies of some ordered smectic phases.¹⁷ Using Eq. (12), $\tau_1 = 1.3 \times 10^{-6}$ sec, and the jump distance $d = 5.03$ Å, we get $D_{\perp} = 0.46 \times 10^{-13}$ m²/sec, which agrees with Krüger's value²⁵ $\langle D \rangle = 0.67 \times 10^{-13}$ m²/sec. Unfortunately, there are no T_{1p} data available so that D_{\parallel} cannot be determined.

In Fig. 13 it is shown how T_1 dispersion in the smectic- B_c phase of the TBBA at 130°C can be similarly explained as in the case of C_{12} BAA with the use of the theory developed in this paper. Here the same $d_{\text{eff}} = 6.9$ Å was used as in the previous case as it cannot be determined by

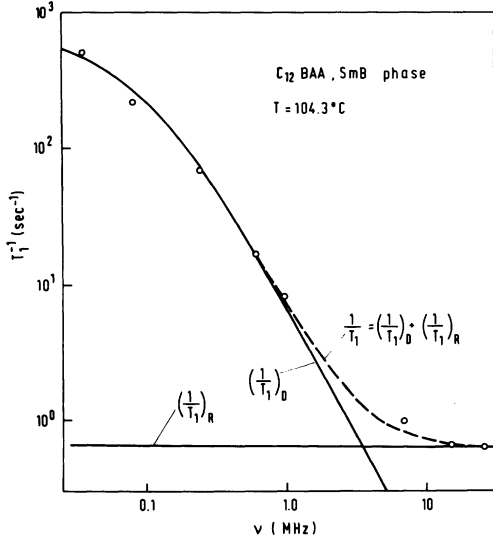


FIG. 12. Frequency dependence of T_1^{-1} in the crystalline- B phase of C_{12} BAA. The dashed curve is the sum of the $(T_1^{-1})_D$ and $(T_1^{-1})_R$.

the high-frequency T_1 data themselves. The best fit is obtained with $\tau_1 = 0.47 \times 10^{-6}$ sec and $(T_1^{-1})_R = 0.32$ sec $^{-1}$ if $l/d \approx 5$ and $n = 0.05$ Å $^{-3}$. Using the lattice constant $d = 5.17$ Å (Ref. 17) for the jump length we find $D_{\perp} = 1.4 \times 10^{-13}$ m 2 /sec which is consistent with the previous evaluation 3,4 of $\langle D \rangle$.

IV. CONCLUSIONS

In this paper the theory of the intermolecular longitudinal spin relaxation due to molecular self-diffusion in the crystalline- B and hexatic- B phases is treated. With the use of the general theory for the diffusion-induced spin relaxation developed in I the effect of 3D ordering of these liquid crystalline systems has been taken into account. Translational diffusion is described by two independent random jump motions, one in the 2D hexagonal lattice and another between the regularly stacked layers.

Numerically evaluated results for T_1^{-1} and $T_{1\rho}^{-1}$ show that at usual NMR frequencies T_1^{-1} due to the translational diffusion in smectic- B phases is expected to be practically isotropic with ω^{-2} type dispersion, while $T_{1\rho}^{-1}$ is expected to be anisotropic with characteristic $c_0 - c_1 \omega_1^{1/2}$ frequency dependence. The comparison between the theoretical prediction for the self-diffusion induced part of T_1^{-1} and experimental data could yield the value of the diffusion constant D_{\perp} in the smectic- B phases which can be—in view of its low value—hardly measured by direct NMR and other methods. The investigations of $T_{1\rho}$ can

$$P_I(\vec{r}, \vec{r}', t) = g_1(\vec{r}') \int G_1(\vec{\rho}, t) G_1(\vec{\rho}_1 + \vec{\rho} - \vec{\rho}', t) \delta(z_1) \delta(z_1 + z - z') e^{-2t/\tau_{\parallel}} d^3 r_1, \quad (\text{A2})$$

where $g_1(\vec{r})$ is given by Eq. (16) and $G_1(\vec{\rho}, t)$ by

$$G_1(\vec{\rho}, t) = \int e^{i\vec{q}_1 \cdot \vec{\rho}} e^{-t[1 - A_1(\vec{q}_1)]/\tau_1} d^2 q_1. \quad (\text{A3})$$

Starting 29 with the expression

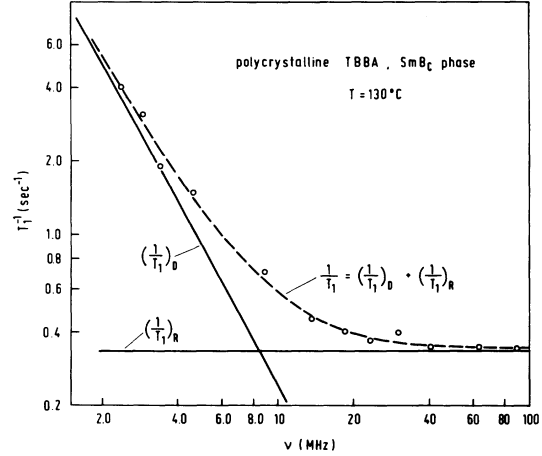


FIG. 13. Frequency dependence of T_1^{-1} in the smectic- B_c phase of TBBA. The dashed curve is the sum of the $(T_1^{-1})_D$ and $(T_1^{-1})_R$.

provide the value of D_{\perp}/D_{\parallel} and promise even an insight into the interlayer correlations.

The theory is used to explain the proton relaxation and to determine D_{\perp} component of the self-diffusion tensor in the smectic- B phase of C_{12} BAA. Further it is proposed that the theory developed for smectic- B phases can be applied to the smectic- B_c phases as well. This is illustrated in the case of TBBA.

APPENDIX

When the modulation of the interlayer magnetic interactions due to relative translational motion of two adjacent smectic layers is fast compared to the modulation induced by translational diffusion, these interactions are motionally averaged on the time scale important for the diffusion part of the relaxation process. The part of the dipolar coupling which is averaged out contributes only to the magnetic spin relaxation caused by the layer sliding. 20 Thus the autocorrelation function of the spatial part of the dipolar interactions $\langle F^{(k)*}(\vec{r}(0)) F^{(k)}(\vec{r}(t)) \rangle$ which is used in the evaluation of T_1^{-1} due to the translational self-diffusion is different from zero only when $\vec{r}(0)$ and $\vec{r}(t)$ are both in the same layer. To describe the intralayer correlations only, a partial one-particle autocorrelation function $G_I(\vec{r}, t)$ is introduced $^{28-30}$:

$$G_I(\vec{r}, t) = \delta(z) e^{-t/\tau_{\parallel}} G_1(\vec{\rho}, t), \quad (\text{A1})$$

where $G_1(\vec{\rho}, t)$ describes the intralayer motion and τ_{\parallel} is the interlayer jump time. Neglecting two-particle dynamical correlations we can introduce the joint probability function $^{28-30}$ $P_e(\vec{r}, \vec{r}', t)$, which describes the relative motion of the two particles, as

$$J^{(k)}(\omega) = \int [F_{\xi}^{(k)*}(\vec{r}) F_{\xi}^{(-k)}(\vec{r}')]_{\xi} P_I(\vec{r}, \vec{r}', t) \times g(\vec{r}) d^3 r d^3 r' e^{i\omega t} dt, \quad (\text{A4})$$

and using Eqs. (A2) and (A3) we can write the spectral

density in the following form:

$$J^{(k)}(\omega) = \frac{n}{4\pi^2} \int [\mathcal{F}_\xi^{(k)*}(\vec{q}_1) \mathcal{F}_{0\xi}^{(k)}(\vec{q}_1)]_\xi \times S_s(\vec{q}_1, \omega/2) d^2q_1, \quad (\text{A5})$$

where $S_s(\vec{q}_1, \omega/2)$ is given by Eqs. (7)–(9) with $A_{||}=0$. Comparing this expression to Eq. (3) one can notice that here $\mathcal{F}_\xi^{(k)}$ and $\mathcal{F}_{0\xi}^{(k)}$ depend only on \vec{q}_1 and that the integration is two dimensional.

- ¹C. G. Wade, *Ann. Rev. Phys. Chem.* **28**, 47 (1977).
²W. Wölfel, *Kernrelaxationsuntersuchungen der Molekülbewegung im Flüssigkristall PAA* (Minerva Publikation, München, 1978).
³R. Blinc, M. Luzar, M. Vilfan, and M. Burgar, *J. Chem. Phys.* **63**, 3445 (1975).
⁴R. Blinc, M. Vilfan, M. Luzar, J. Seliger, and V. Žagar, *J. Chem. Phys.* **68**, 303 (1978).
⁵Th. Mugele, V. Graf, W. Wölfel, and F. Noack, *Z. Naturforsch.* **35a**, 924 (1980).
⁶M. Vilfan, J. Seliger, V. Žagar, and R. Blinc, *Phys. Lett.* **79A**, 186 (1980).
⁷G. J. Krüger, H. Spiesecke and R. Steenwinkel, *J. Phys.* **37**, 123 (1976); G. J. Krüger, H. Spiesecke, R. Steenwinkel, and F. Noack, *Mol. Cryst. Liq. Cryst.* **40**, 103 (1977).
⁸R. Blinc, M. Luzar, M. Mali, R. Osredkar, J. Seliger, and M. Vilfan, *J. Phys. (Paris) Colloq.* **37**, C3-73 (1976).
⁹R. Y. Dong, *J. Mag. Res.* **48**, 280 (1982).
¹⁰M. Kosterlitz and D. J. Thouless, *J. Phys. C* **6**, 1181 (1973).
¹¹B. I. Halperin and D. R. Nelson, *Phys. Rev. Lett.* **41**, 121 (1978); D. R. Nelson and B. I. Halperin, *Phys. Rev. B* **19**, 2457 (1979).
¹²R. J. Birgeneau and J. D. Litster, *J. Phys. (Paris) Lett.* **39**, L399 (1978).
¹³A. J. Leadbetter, J. C. Frost, and M. A. Mazid, *J. Phys. (Paris) Lett.* **40**, 325 (1979).
¹⁴D. E. Moncton and R. Pindak, *Phys. Rev. Lett.* **43**, 701 (1979).
¹⁵R. Pindak, D. E. Moncton, J. C. Davey, and J. W. Goodby, *Phys. Rev. Lett.* **46**, 1135 (1981).
¹⁶A. M. Levelut, J. Doucet, and M. Lambert, *J. Phys. (Paris)* **35**, 773 (1974).
¹⁷A. M. Levelut, F. Moussa, J. Doucet, J. J. Benettar, M. Lambert, and B. Dorner, *J. Phys. (Paris)* **42**, 1651 (1981).
¹⁸M. Cagnon, J. F. Paliene, and G. Durand, *Mol. Cryst. Liq. Cryst.* **82**, 185 (1982).
¹⁹Y. Thiriet and P. Martinoty, *J. Phys. (Paris) Lett.* **43**, 137 (1982).
²⁰S. Žumer, *Phys. Rev. A* **15**, 378 (1977).
²¹J. Doucet, *J. Phys. (Paris) Lett.* **40**, 185 (1979).
²²R. Bruinsma and G. Aeppli, *Phys. Rev. Lett.* **48**, 1625 (1982).
²³A. J. Dianoux and F. Volino, *J. Phys. (Paris)* **40**, 181 (1979).
²⁴A. Buka, L. Bata, K. Pinter, and J. Szabon, *Mol. Cryst. Liq. Cryst.* **72**, 285 (1982).
²⁵G. J. Krüger, *Phys. Rep.* **82**, 259 (1982) and references therein.
²⁶J. A. Leadbetter, R. M. Richardson, and J. C. Frost, *J. Phys. (Paris) Colloq.* **40**, C3-125 (1979); R. M. Richardson, A. J. Leadbetter, C. J. Carlie, and W. S. Howell, *Mol. Phys.* **35**, 1697 (1978).
²⁷A. V. Chadwick and M. Paykary, *Mol. Phys.* **32**, 637 (1980).
²⁸S. Žumer and M. Vilfan, *Phys. Rev. A* **17**, 424 (1978).
²⁹H. C. Torrey, *Phys. Rev.* **92**, 962 (1953); H. A. Rhesing and H. C. Torrey, **131**, 1102 (1963); G. Held and F. Noack, *Proceedings of the 8th Congress Ampère, Nottingham, 1974* (Nottingham Ampère Committee, Nottingham, 1974), p. 461.
³⁰M. Vilfan and S. Žumer, *Phys. Rev. A* **21**, 672 (1980).
³¹D. Wolf, *Spin-Temperature and Nuclear-Spin Relaxation in Matter* (Clarendon, Oxford, 1979).
³²A. Abragam, *The Principles of Nuclear Magnetism* (Clarendon, Oxford, 1962); M. Goldman, *Spin Temperature and Nuclear Magnetic Resonance in Solids* (Clarendon, Oxford, 1970).
³³P. S. Hubbard, *Phys. Rev.* **128**, 650 (1962).
³⁴S. Chandrasekhar, *Rev. Mod. Phys.* **15**, 1 (1943).
³⁵C. A. Sholl, *J. Phys. C* **14**, 447 (1981).